

# Prediction of pain duration and pain intensity from patellofemoral pain maps using a deep learning approach

BIRGITHE KLEEMANN RASMUSSEN, IGNAS KUPCIKEVIČIUS,  
LINETTE HELENA POULSEN, MAD S KRISTENSEN

Aalborg University

December 20, 2017

## Abstract

**Introduction:** Patellofemoral pain (PFP) syndrome is a musculoskeletal condition that presents as pain behind or around the patella without known structural changes [1]. Partial correlations between perceived size of PFP from pain maps and pain duration along with pain intensity has been indicated in previous studies [2], however morphology and location of PFP remains unexplored in terms of correlation. Based on the object detection capabilities of deep learning methods can be used to detect image-features related to morphology and location. The aim of this study was to determine the performance of deep learning models for predicting pain duration and pain intensity, based on morphology and location of perceived PFP from pain maps.

**Methods and materials:** PFP drawings were collected on a body-schema and encoded into three different pain map representations in respect of morphology of pain, location of pain, and a combination of morphology and location. The distribution of the outputs were analysed and used for defining the classification intervals for pain duration, to which the intervals were below 12 months and above 36 months, and pain intensity, below 4 and above 8 on VAS. Estimation of generalization performance of the models was calculated during the training.

**Results:** The results during training showed a higher accuracy for pain intensity classification than pain duration classification using morphology-representation. Pain intensity had an accuracy on 65.04%, and pain duration had an accuracy on 59.51%. Furthermore, the combined-representation performed with the highest accuracy on 65.14%. The location and morphology-representation scored 63.33%, and 65.04%, respectively, based on pain intensity.

**Discussion:** Despite pain intensity being defined as multidimensional and subjective, the performance accuracy were higher than that of pain duration. The results may indicate that a combination of the morphology and the location of the pain had a higher classification performance in relation to pain duration or intensity. Currently, it is unclear if deep learning methods may be a suitable approach for classifying PFP syndrome to work as support in clinical settings, to which further investigation is necessary. Improvements could be found when more data become available to better reflect generalization patterns in PFP drawings.

## I. INTRODUCTION

Patellofemoral pain (PFP) syndrome is a painful musculoskeletal condition that is presented as pain behind or around the patella [1, 2]. PFP syndrome affects 6-7% of adolescents, of whom two thirds are highly physically active [3]. Additionally, the prevalence is more than twice as high for females than males [3, 4]. PFP syndrome is typically present over a longer period of time where a high number of individuals experience a recurrent or chronic pain [5]. Chronic pain may be maintained by the phenomenon central sensitization, which may result in widespread pain over time.

Ultimately, PFP syndrome may lead to osteoarthritis [4, 6].

PFP is often described as diffuse knee pain, that can be hard for individuals to explain and localize [5]. Despite that individuals feel pain in the knee, there is no underlying structural changes in the knee such as significant chondral damage. There is no definitive clinical test to diagnose PFP syndrome and is often diagnosed based on exclusion criterias [4], to which PFP syndrome is also described as an orthopaedic enigma, and is one of the most challenging pathologies to manage [7]. To assist diagnosis of PFP syndrome, pain maps may be used as a helpful tool for the individuals

to communicate their pain by drawing pain areas on a body outline [8].

A study by Boudreau et al. [9] indicates, through the use of pain maps (n=35), that there is a correlation between the size of the pain areas (total number of pain pixels) and the pain duration as well as pain intensity for individuals with PFP duration longer than five years.[9] However, it is unknown whether pain duration has an influence on morphology of the pain and location, as well as whether morphology of pain and location have an influence on pain intensity. The relation between pain maps and pain duration or pain intensity may be complex, because the perceived PFP is subjective, and considered as multifactorial [10]. Additionally, the study by Boudreau et al. [9] did not find a correlation between 35 pain maps and pain duration or pain intensity for individuals with a pain duration below 5 years. To investigate the potential nonlinear correlation, a deep learning method was used, which previously has not been applied on this type of data. The goals of this study was to explore how accurate a deep learning model can classify pain maps according to pain duration or pain intensity. It was assumed that pain duration would be a better predictor than pain intensity, because of the subjectivity of pain, and its possibility of being multifactorial. The pain maps were encoded into multiple pain map representations to investigate whether morphology of the pain or location were correlated to pain duration or pain intensity.

It is assumed that a deep learning model will perform better with more features, thus a combined-representation containing morphology and location of the pain was made. The representations are referred to as morphology- (MR), location- (LR), and combined-representation (CR). The aim of this study was to explore classification performance of deep learning models, using PFP maps as input to classify according to either pain duration or pain intensity, and to compare performance accuracy between the three pain map representations (MR, LR, and CR).

## II. METHODS

This section presents the pain maps and the pre-processing. Furthermore, the multiple pain map representations are described, whereafter the linearity of the pain maps is investigated. Finally, the deep learning architectures are presented.

### Pain maps

Pain maps used in this study were collected from an on-going clinical trial (FOXH) which is conducted in collaboration with Danish and Australian universities. The pain maps were drawn by individuals with PFP syndrome through the use of an application, Navigate Pain, in a clinical setting.

Navigate Pain is a software application that is used to visualize the location, morphology, and spatial distribution of pain from individuals to healthcare personnel. The application permits individuals to draw their pain with different colors and line thickness onto a body outline, an example is shown in fig. 1. Navigate Pain was developed at Aalborg University.[12]



**Fig. 1:** Pain maps from individuals with uni- and bilateral PFP. The red markings indicate the area of pain perceived by the individuals.

The number of pain maps associated with pain duration was 205, and 197 associated to pain intensity measured according the Visual Analog Scale (VAS). The gender was included as an input, because females may report a more intense and frequent pain than males [11], with the intentions of making the deep learning models better at classifying the pain maps.

### Pre-processing

The pain maps were processed in MatLab v. R2017b, where the images were resized, since they were collected at different resolutions (screen sizes) and cropped to only include the knees. To create more pain maps a split body approach was used, where the two knees in the pain maps were separated into

individual images. The left knee was then mirrored to resemble the right knee to minimize the variance in the images. The final pain maps had a pixelsize of  $252 \times 118$ . By using split body approach it was assumable that the pain duration and pain intensity were identical for both knees if PFP was bilateral. This resulted in an increased total number of pain maps with gender and pain duration to 333, and pain maps with gender and pain intensity to 319, of which 15% was used as test data, and therefore not used to optimize and train the deep learning models.

The models were designed to classify pain maps according to pain duration or pain intensity divided into two classes with intervals based on the extremes. The classification intervals were 0 to 12 months and 36 to 300 months for pain duration, and 0 to 4 and 8 to 10 for pain intensity measured on VAS. The reason for choosing extreme intervals, was to separate closely related patterns between the two classes.

### Morphology-representation

The original pain maps reflect the morphology of the pain, and did not require further processing than converting the pain maps to a matrix including gender and the output, pain duration or pain intensity. As a result of using only the extremes for classifying, the number of pain maps decrease to 236 for pain duration, and 196 for pain intensity.

### Pain location

The knee was divided into regions based on the underlying anatomical structures, which may have a correlation to pain duration or pain intensity. The locations were divided into 10 regions, which were inspired by Photographic Knee Pain Map (PKPM). The divisions were designed to categorize location of knee pain for diagnostic and research purposes.[13] The knee regions are illustrated in fig. 2.

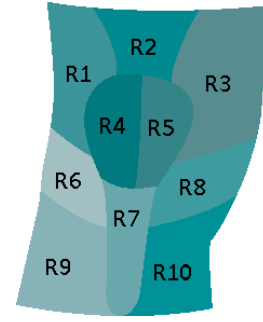
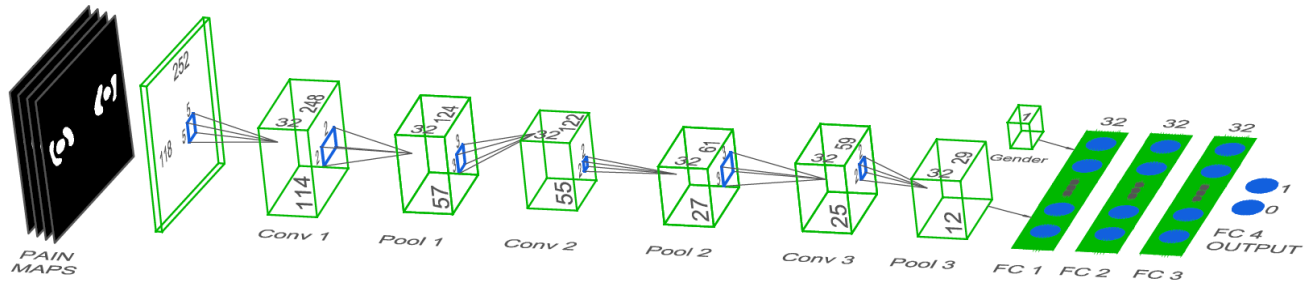


Fig. 2: The regions of the right knee (R1-R10).

There are ten regions, where regions 1 and 3 represent the superior lateral and superior medial areas for patella. Region 2 refers to quadriceps tendon. The patella is divided into lateral and medial regions, which are regions 4 and 5. Regions 6 and 8 are lateral and medial joint line areas. Patella tendon is region 7 and the two last regions, 9 and 10, are tibia lateral and medial.[13]

### Location-representation

A simplified representation of the pain maps was created to investigate whether the location have patterns related to the pain duration or pain intensity. The location of the pain was reflected by the use of the defined knee regions (fig. 2), where a 10 elements vector were created. Each value represented either an active region (1) or a not active region (0). The values were defined by using a threshold to determine whether a region was considered active in relation the amount of pain in the specific region. A threshold was required to increase the confidence of an active pain region by avoiding minimal contributions. Simultaneously, the threshold should not be too high to avoid excluding too many or big areas. The threshold indicated which minimal percentage of pain pixels, that should be present in a specific region before it was considered as active. The threshold was decided based on an analysis on five random pain maps, where threshold values of 0, 5, 10 and 15% was compared. Based on the analysis, a 5% threshold was chosen. As a result of using the extremes for classification, and adding the threshold value, the number of pain maps with pain duration decreased to 223, and the number of pain maps with pain intensity decreased to 186.



**Fig. 3:** The architecture of the deep learning models including the morphology-representation before optimization. The models consisted of three convolutional, three max pooling, and four fully connected layers. The gender was included in the first fully connected layer. The boxes represented the output after each layer.

### Combined-representation

A combination of morphology and location of the pain was created based on components from MR and LR. The original pain maps were superimposed on the knee regions, which resulted in pain pixels reflecting the location with a number from 1 to 10. Before using the representation as input in the deep learning models, a one-hot encoding approach was used, which made it possible to separate categorical data into binary data [14]. As a result, the 10 values did not have a relation to each other when analysed in the deep learning models. By classifying according to the extremes, the number of pain maps decreased to 234 for pain duration, and 194 for pain intensity.

### Nonlinearity in pain maps

Given that PFP is subjective and multifactorial it is unlikely that the pain maps and pain duration or pain intensity are linearly correlated. In order to determine if there was a linear relationship, linear regressions were done on simple features reflecting the size of the pain and number of active pain regions. Linear regressions were made in MatLab, and composed correlations between; number of pain pixels and pain duration, number of pain pixels and pain intensity, number of active pain regions and pain duration, and number of active pain regions and pain intensity.

### Architecture of the deep learning models

Deep learning models were developed on a computer with 4x "Intel® Core™ i7" CPUs and one single GPU of type "Geforce GTX 970M", using the programming language Python v3.6.3. Libraries used was Keras

v2.0.8 with a TensorFlow v1.3.0 backend.

Six deep learning models suitable to the three pain map representations and pain duration or pain intensity were created. The models used supervised learning, which is defined as a network learning to classify a given input corresponding to a specific output [15]. The models were designed differently according to each pain map representation and type of classification. The architecture of the models, before optimization, including the MR is illustrated on fig. 3. The models classified MR and CR consisted of three convolutional layers, to which a max pooling layer was added after each convolutional layer, and followed by four fully connected layers, where gender was inserted as a secondary input for the models. The only difference in the models using the CR was the input image, which was represented a matrix with 10 layers. The models including the LR consisted of only four fully connected layers of the architecture shown in fig. 3.

### The convolutional layers

Convolutional Neural Networks (CNNs) is a type of neural network for processing data with a grid-like topology [15]. CNNs were used to the MR and CR because of its capability to perform highly according to image classification. The purpose of the convolutional layers was to recognize the features in the pain maps by taking the image and scan it, then split it up into feature maps.[15, 16] The architecture of the first convolutional layer consisted of a kernel size on  $5 \times 5$ , and 32 filters. The two following convolutional layers consisted of kernel sizes on  $3 \times 3$ , and 32 filters.

### Max pooling layers

For the models containing convolutional layers, each convolution layer was followed by a max pooling layer, which is a typical structure of a convolutional network [15, 17]. Max pooling layers are used to reduce the size of the dataset, while maintaining features from the feature maps. Given a reduction in the data, the computation speed may increase.[15, 16] Max pooling layers were defined after each convolutional layer, to which all have a kernel size of  $2 \times 2$  with a stride of 2. From the kernel window the highest of the 4 values was extracted to next layer, and used further through the network.

### Fully connected layer and output layer

The models consisted of four fully connected layers, where the first layer received a flattened version of the input. The notation for gender was included in the end of the array, which was used as input in the first fully connected layer with 32 nodes. Additionally, the second and third layers consisted of 32 nodes. The fourth fully connected layer, which also was the output layer, included a sigmoid activation function. This function operates with a single output, that saturates when its input is either extremely negative or extremely positive [15]. The single output refers to the number of classification intervals, pain duration below 12 month, and above 36 month, or pain intensity below 4, and above 8 on VAS.

### ReLU activation function

The activation function, chosen for all hidden layers in the models, was Rectified Linear Unit (ReLU), which transforms the linear output to a nonlinear function by making all negative values to zero. The ReLU function still remains nearly linear, which means it can easily be optimized with gradient descent based methods. In modern neural networks, ReLU is recommended to use as a default activation function and could be defined as  $g(x) = \max\{0, x\}$ . [15]

### Dropout algorithm

A dropout algorithm was implemented for the models in the first two hidden fully connected layers to reduce overfitting while training. The algorithm works by randomly dropping a specified fraction of the nodes in the given layer, to which the nodes that drop, and

changes between different nodes during the training [18]. Dropout reduce the nodes' ability for co-adaptation, where multiple nodes compute the same features. For the models the dropout fraction was set to 0.5 (50%) based on a previous study by Srivastava et al. [18], which found 0.5 as optimal for multiple range of networks.

### Back-propagation algorithm

Back-propagation was used for the learning process where the weights of the models were adjusted in order to reduce the error calculated between the predicted output, and the correct output [19]. Back-propagation is based on gradient descents, which computes gradients from the output to the input, in order to minimize the overall output error as much as possible during the learning stage. After each pass of a minibatch, the inputs and weights were multiplied for each node summed with additional coefficient bias.[16, 20] Afterwards, a loss was calculated based on a loss function for every input that passed through the network to make the adjustments on the parameters to reduce the loss. As training progressed, the loss should decrease as a result of the parameter updates, and improve the performance of the neural network.[15, 17, 19] This learning process continued until optimal parameters with minimum error were reached.[20]

### Training

The models were trained and optimized with a structured grid search on the hyperparameters to help set the initial parameters for the models. These hyperparameters refer to learning rate, kernel initializer, number of filters and nodes, and number of epochs with different batch sizes. Accuracy was used to determine the improvement of performance when testing the multiple parameters. Further manual optimization was performed by evaluating the development in loss, and accuracy during training, and the general performance estimated from an accuracy, sensitivity, and specificity. After optimization, the models were trained anew using all of the training data (n=85%), using the optimal hyperparameters from training, and then tested with a separate test subset (n=15%).

### III. RESULTS

This section visualizes the results from the linear regressions, and performance of the deep learning models using multiple pain map representations, and different outputs.

#### Linear correlations

The linear regression between simple features, number of pain pixels or active pain regions, and outputs, pain duration or pain intensity, resulted in the plots shown in fig. 4. The  $R^2$ -values support the nonlinearity, shown in the plots, where correlation fig. 4a resulted in a  $R^2 = 0.018$ , fig. 4b resulted in  $R^2 = 0.008$ , fig. 4c resulted in  $R^2 = 0.011$  and fig. 4d resulted in  $R^2 = 0.011$ .

#### Optimization of the models

During the optimization, a structured grid search resulted in different hyperparameters according to each model. The learning rate was different for the models including MR according to pain duration (0.02), and pain intensity (0.1). An optimization in kernel initializer was defined as glorot\_uniform for pain duration, and glorot\_normal for pain intensity. The nodes were changed from 32 in the fully connected layers to 64 for pain duration, and 16 for pain intensity. Lastly, an optimization was made for number of epochs, and batch size, which were changed to 120 and 20 for pain duration, and 140 and 10 for pain intensity. The models including the LR had similar results from the optimization. A learning rate of 0.01, a glorot\_uniform kernel initializer, 16 nodes, and number of epochs

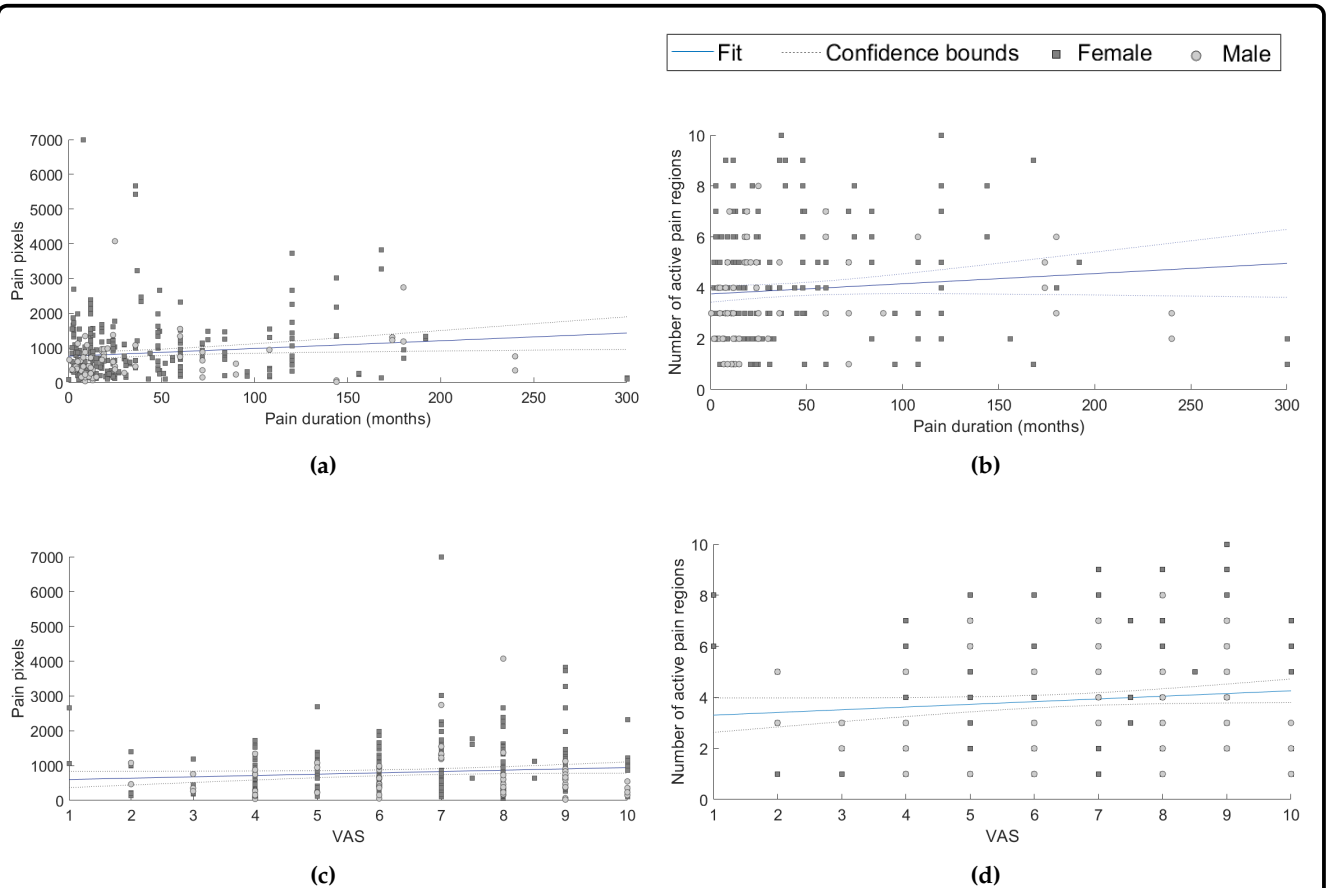


**Fig. 4:** Linear correlations of pain pixels and pain duration (a), active pain regions and pain duration (b), pain pixels and pain intensity indicated in VAS (c), and active pain regions and pain intensity indicated in VAS (d).

and batch size of 120 and 20. Results of optimization on the models including the CR were almost identical. Both resulted in the best performance with a glorot\_uniform kernel initializer, 16 nodes, and with a number of epochs and batch size of 120 and 30, to which the only difference was in the learning rate that for pain duration was 0.1, and 0.001 for pain intensity.

tensity, confusion matrices were created, and is shown in fig. 5.

## Performance of the models

The average performance accuracy, sensitivity, and specificity of the models during test with new pain maps in different representations are shown in tab. 1. For the pain map representations that resulted in the highest accuracy for either pain duration or pain in-

	Avg. accuracy (%)	Avg. sensitivity (%)	Avg. specificity (%)
Morphology-representation			
Pain duration	69.44%	69.23%	69.57%
Pain intensity	60.00%	40.00%	70.00%
Location-representation			
Pain duration	35.29%	0.00%	35.29%
Pain intensity	60.71%	0.00%	60.71%
Combined-representation			
Pain duration	55.56%	61.11%	50.00%
Pain intensity	73.33%	0.00%	73.33%

**Table 1:** Generalization performance of the models, which use the MR, LR, and CR when classifying according to pain duration or pain intensity.

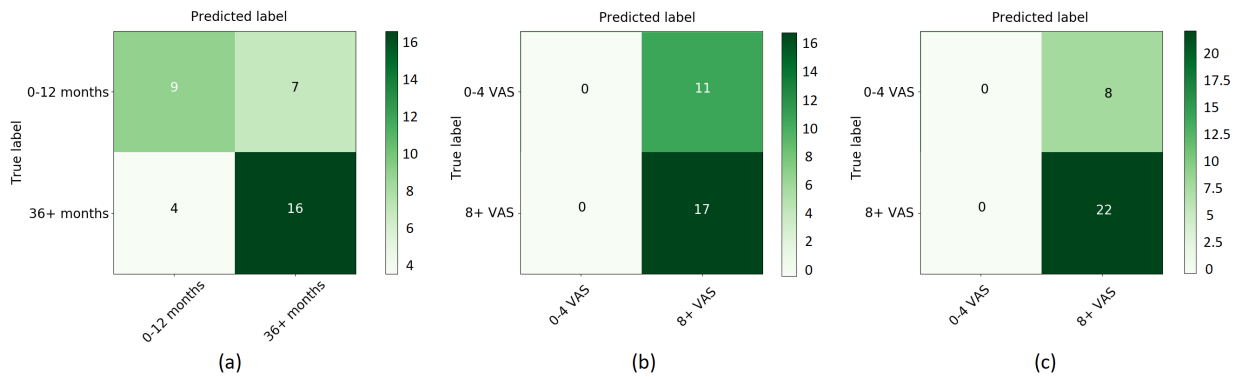


**Fig. 5:** Confusion matrices of (a) MR classified according pain duration, (b) LR classified according to pain intensity, and (c) CR classified according to pain intensity.



## IV. DISCUSSION

This section discusses complexity of pain maps, and what may optimize the performance of the models. Furthermore, the results are discussed, whereas the highest performance value of the pain maps representations is evaluated. Finally, the performance according to the output, pain duration or pain intensity, is discussed.

### Amount of pain maps

In this study the total number of pain maps was 217 from individual with uni- and bilateral PFP. Comparing to the literature, a supervised deep learning model should use five thousand labeled data per category to obtain an acceptable performance [15]. The amount of pain maps was not optimal, to which a split body approach was used to compensate this. During this approach combined with the mirroring pain to the right knee, it was assumed that pain duration and pain intensity were identical for both knees. Theoretically, the bilateral PFP may have occurred on one leg first, and afterwards have spreaded to the other knee, which could affect the pain duration. Furthermore, individuals with bilateral pain may feel more pain on one of the knees. This may have resulted in incorrect labeled pain maps, which could influence the performance accuracy of the models.

### Classification of pain maps

The  $R^2$ -values of the linear correlations were close to zero, which represents nonlinearity, meaning that there are no simple correlation between the simple features and the outputs, pain duration and pain intensity. Thus, a deep learning model is used to investigate the complexity of pain maps. The deep learning models could classify both pain duration and pain intensity classes in the MR. Models including LR classified only according to the higher intervals (pain duration above 36 months and pain intensity above 8 VAS), and appears unable to classify according to the lower classes (pain duration below 12 month and pain intensity below 4 VAS). This can be observed in the confusion matrices of LR, where sensitivity of both inputs were equal to 0%. CR, classified according to the pain duration, found the patterns in both classes, but overall accuracy was 55.56%, which could be caused by in-

cluding the knee regions as one of the features. Based on the results, the accuracy of MR, scored higher compared to LR. It can be discussed, that the morphology can be considered to be a better classification feature. Models containing MR scored 69.44% and 60% while LR scored 35.29% and 60.71%, reflecting pain duration and pain intensity. Low score in LR could be considered as a result of imbalance between the duration intervals, as it could be also influenced with a further optimization. The low score could also be the result of the simplification of the location of the pain, that leads to the models not being able to find a pattern between the input and target output.

### Threshold

The LR had a 5% threshold that defined when a pain region was considered active according to the amount of pain. It can be discussed whether this threshold was suitable, since adding the threshold resulted in loss of pain maps that had a very small amount of pain. However, a smaller threshold or no threshold would give active pain regions that might only contain very few pain pixels. Since PFP is described as hard to localize, it is unknown how precise the individuals have drawn their pain, thus every pixel should maybe not be taken into account. The CR did not have a threshold for defining active pain regions, because the morphology of the pain would be affected when discarding small pain regions. This representation is not a complete combination of the MR and LR.

### Classification according to output

Generalization performance of the six models showed that pain duration was a more stable classifier compared to pain intensity. As a result, both classes of pain duration can be predicted in the MR and CR, while classes representing pain intensity can be classified only with the morphology-representation. It could be discussed that the lower results of pain intensity against the pain duration, might be caused by that the pain intensity is a subjective statement and is considered as multifactorial, while pain duration is an objective parameter, and it is thereby expected that the models have a higher performance when classifying pain maps according to pain duration. Given the fact that the sensitivity for multiple models was 0%, the accuracy becomes a reflection of the imbalance between



classes in the test set, e.g. if the test subset contained 75% of the class with high pain intensity, the accuracy would also be 75%. This may also be a result of the limited amount of pain maps used in this study. It is unknown whether the reason for the sensitivity to be 0% is caused by that the models cannot find patterns according to the low valued pain intensity (0 to 4 VAS), or it could be a result of the models being poor, and classifies all inputs as high pain intensity (8 to 10 VAS).

## Optimization of deep learning models

Optimization of the deep learning models is often a time-consuming process based on the picks of the multiple hyperparameters and different algorithms which could be implemented during the development of the models. Activation functions were chosen based on the literature, where ReLU should be used for convolutional and fully connected layers in neural network models, and sigmoid should be picked for binary output layer. However, additional testing could be made by using softmax or linear activation function to increase the generalization performance. The dropout algorithm was set to the default 0.5 and used in all models between the fully connected layers to turn off the amount of nodes and prevent the models from overfitting. Additional values could have been tested in order to find most optimal for the every model. Unfortunately, the lack of time and time-consuming reruns during every optimization cycle, lead to use the common hyperparameters as there were many other which were tested with grid search 10-fold cross validation. A limitation for this study was the available computational power for training of the model to which an improvement in performance may be found through more powerful systems or services.

A further optimization of the models may be found according to the input parameters, to which more physical, and psychological features may increase the performance accuracy. Physical features, such as age, height, weight, physical activity level, and sport activity, may influence pain duration or pain intensity. Age could be a relevant feature since the perceived pain is dependent on the individual's personality and character. Younger individuals may feel more pain because of a new pain, than older individuals which have had PFP for a longer period of time. In addition, older individuals may feel more pain because of the phenomenon central sensitization, which in some

cases results in widespread pain. The physical activity level, and sport may increase the pain intensity for some individuals because of the patellofemoral loaded activity. Psychological factor is an important feature to consider, because of its influence on pain intensity. Pain is multifactorial and can be influenced of psychosocial factors [21]. Furthermore, other pain areas, such as hip pain, may influence the pain intensity of PFP. It may be considered to include either pain duration or pain intensity as an input to classify according to either pain intensity or pain duration, because of the possibility that there is a correlation between the two.

## V. CONCLUSION

During this study the deep learning models were presented for classifying pain maps according to the pain duration or pain intensity. The overall performance of the models were calculated, to which the CR performed with the highest accuracy, but the models using the MR resulted as the most reliable classifier based on the sensitivity and specificity. There may be an indication of a pattern to be found between pain maps and pain duration or pain intensity, however further optimization or additional studies is needed to support whether location or morphology contains positive predictive value in terms of classifying pain duration or pain intensity.

WHICH ONE IS BEST!

## REFERENCES

- [1] Liam R. Maclachlan, Natalie J. Collins, and Et.al. The psychological features of patellofemoral pain: a systematic review. 2017. doi: 10.1136/bjsports-2016-096705.
- [2] T.O. Smith, B.T. Drew, and Et.al. Knee orthoses for treating patellofemoral pain syndrome (review). 2015. doi: 10.1002/14651858.CD010513.pub2.
- [3] M. S. Rathleff, B. Vicenzino, and Et.al. Patellofemoral Pain in Adolescents and adulthood: same same, but different? 2015. doi: 10.1007/s40279-015-0364-1.
- [4] Amir Haim, Moshe Yaniv, and Et.al. Patellofemoral Pain Syndrome. *Knee Surg sports traumatol arthrosc*, 451:223–228, 2006. ISSN 0009-921X. doi: 10.1007/s00167-013-2759-6. URL <http://content.wkhealth.com/linkback/openurl?sid=WKPTLP:landingpage{&}an=00003086-200610000-00041>.
- [5] Erik Witvrouw, Michael J. Callaghan, and Et.al. Patellofemoral Pain: consensus statement from the 3rd International Patellofemoral Pain Research Retreat held in Vancouver, September 2013. 2014. doi: 10.1136/bjsports-2014-093450.

- [6] Kay M. Crossley, Michael J. Callaghan, and Et.al. Patellofemoral pain. 2016. doi: 10.1136/bjsports-2015-h3939rep.
- [7] Scott F Dye. Patellofemoral Pain Current Concepts: An Overview. *Sports Medicine and Arthroscopy Review*, 2001.
- [8] Shellie A. Boudreau, Susanne Badsberg, and Et.al. Digital pain drawings: Assessing Touch-Screen Technology and 3D Body Schemas. 2016. doi: 10.1097/AJP.0000000000000230.
- [9] Shellie A. Boudreau, E. N. Kamavuako, and Et.al. Distribution and symmetrical patellofemoral pain patterns as revealed by high-resolution 3D body mapping: a cross-sectional study. 2017. doi: 10.1186/s12891-017-1521-5.
- [10] E. J. Dansie and D. C. Turk. Assessment of patients with chronic pain. 2013. doi: 10.1093/bja/aet124.
- [11] Christoph Pieh, Jurgen Altmeyen, and Et.al. Gender differences in outcomes of a multimodal pain management program. *Elsevier*, 2012. doi: 10.1016/j.pain.2011.10.016.
- [12] Aglance Solutions. Visual insight for clinical reasoning – Navigate Pain, 2015. URL <http://www.navigatepain.com/>.
- [13] D. W. Elson, S. Jones, and Et.al. The photographic knee pain map: Locating knee pain with an instrument developed for diagnostic, communication and research purposes. 2010. doi: 10.1016/j.knee.2010.08.012.
- [14] David Money Harris and Sarah L. Harris. Sequential Logic Design. In *Digital design and computer architecture*. Elsevier, 2012. ISBN 9780123978165.
- [15] Ian Goodfellow, Yoshua Bengio, and Et.al. *Deep Learning*. MIT Press, 2016. URL <http://www.deeplearningbook.org>.
- [16] Yann LeCun, Léon Bottou, and Et.al. Gradient-based learning applied to document recognition. *Proceedings of the IEEE*, 86(11):2278–2323, 1998. ISSN 00189219. doi: 10.1109/5.726791. URL <http://yann.lecun.com/exdb/publis/pdf/lecun-01a.pdf>.
- [17] Yann LeCun, Yoshua Bengio, and Et.al. Deep Learning. *Nature Insight Review*, pages 436–444, 2015. doi: 10.1038/nature14539. URL <https://www.nature.com/nature/journal/v521/n7553/pdf/nature14539.pdf>.
- [18] Nitish Srivastava, Geoffrey Hinton, and Et.al. Dropout: A Simple Way to Prevent Neural Networks from Overfitting. *Journal of Machine Learning Research*, 15:1929–1958, 2014. ISSN 15337928. doi: 10.1214/12-AOS1000. URL <https://dl.acm.org/citation.cfm?id=2670313&CFID=818407627&CFTOKEN=74532044>.
- [19] Richard Duda, Peter Hart, and Et.al. *Pattern Classification*. Second edition, 2000. ISBN 9780471056690.
- [20] Alaa Ali Hameed, Bekir Karlik, and Et.al. Back-propagation algorithm with variable adaptive momentum. *Knowledge-Based Systems*, 114: 79–87, 2016. ISSN 09507051. doi: 10.1016/j.knosys.2016.10.001. URL <http://www.sciencedirect.com/science/article/pii/S0950705116303811?via=ihub>.
- [21] Ewa M. Roos and L. Stefan Lohmander. The knee injury and osteoarthritis outcome score (KOOS): from joint injury to osteoarthritis. *Bio Med Central*, 2003.